Design and Evaluation of Electrotactile Rendering Effects for Finger-Based Interactions in Virtual Reality

Sebastian Vizcay, Panagiotis Kourtesis, Ferran Argelaguet, Claudio Pacchierotti, Maud Marchal

Design and Evaluation of Electrotactile Rendering Effects for Finger-Based Interactions in Virtual Reality

Sebastian Vizcay
sebastian.vizcay@inria.fr
Inria, Univ Rennes, IRISA, CNRS
Rennes, France

Panagiotis Kourtesis
panagiotis.kourtesis@inria.fr
Inria, Univ Rennes, IRISA, CNRS
Rennes, France

Ferran Argelaguet
ferran.argelaguet@inria.fr
Inria, Univ Rennes, IRISA, CNRS
Rennes, France

Claudio Pacchierotti
claudio.pacchierotti@irisa.fr
CNRS, Univ Rennes, Inria, IRISA
Rennes, France

Maud Marchal
maud.marchal@irisa.fr
Univ Rennes, INSA, IRISA, Inria,
CNRS and IUF
Rennes, France

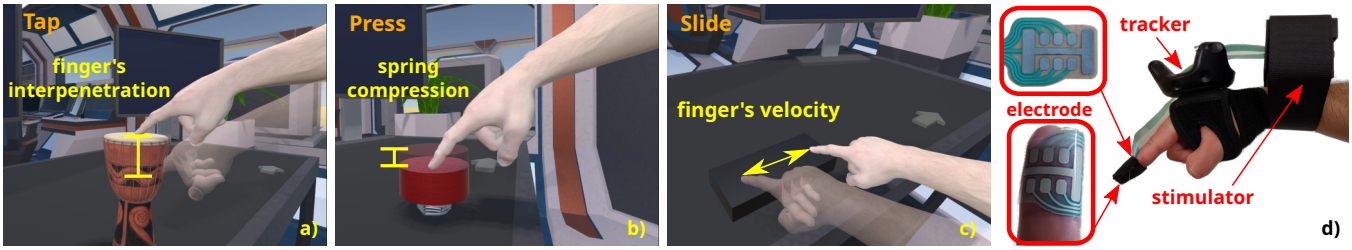

Figure 1: The three left-most figures (a)-(c) illustrate the tree evaluated interaction tasks: tapping, pressing and sliding. The right-most figure (d) illustrates the electrotactile equipment used in the experiment, the inset shows the electrode layout.

ABSTRACT

The use of electrotactile feedback in Virtual Reality (VR) has shown promising results for providing tactile information and sensations. While progress has been made to provide custom electrotactile feedback for specific interaction tasks, it remains unclear which modulations and rendering algorithms are preferred in rich interaction scenarios. In this paper, we propose a unified tactile rendering architecture and explore the most promising modulations to render finger interactions in VR. Based on a literature review, we designed six electrotactile stimulation patterns/effects (EFXs) striving to render different tactile sensations. In a user study (N=18), we assessed the six EFXs in three diverse finger interactions: 1) tapping on a virtual object; 2) pressing down a virtual button; 3) sliding along a virtual surface. Results showed that the preference for certain EFXs depends on the task at hand. No significant preference was detected for tapping (short and quick contact); EFXs that render dynamic intensities or dynamic spatio-temporal patterns were preferred for pressing (continuous dynamic force); EFXs that render moving sensations were preferred for sliding (surface exploration). The results showed the importance of the coherence between the modulation an the interaction being performed and the study proved the versatility of electrotactile feedback and its efficiency in rendering different haptic information and sensations.

CCS CONCEPTS

• **Human-centered computing** → **Haptic devices**; **Virtual reality**.

KEYWORDS

electrotactile feedback, virtual reality, human computer interaction

ACM Reference Format:
Sebastian Vizcay, Panagiotis Kourtesis, Ferran Argelaguet, Claudio Pacchierotti, and Maud Marchal. 2022. Design and Evaluation of Electrotactile Rendering Effects for Finger-Based Interactions in Virtual Reality. In *28th ACM Symposium on Virtual Reality Software and Technology (VRST '22), November 29-December 1, 2022, Tsukuba, Japan.* ACM, New York, NY, USA, 11 pages. https://doi.org/10.1145/3562939.3565634

1 INTRODUCTION

In Virtual Reality (VR), a realistically reactive environment is necessary for inducing a plausibility illusion, and strengthen the sense of presence [38]. Specifically, while interacting in VR, matching user's expectations increases the sense of presence [37] and the sense of agency [18]. In this direction, the addition of kinesthetic and tactile feedback (haptic feedback) is paramount in naturalistic mid-air interactions [28, 32]. As such, the use of wearable devices has been widely explored as they provide a cost-effective solution to provide rich tactile feedback with a reduced form factor [10, 29, 36, 39].

However, different devices can be required to provide rich tactile sensations and/or haptic information [2], which could also suffer from decreased portability and wearability [8, 27, 29].

Electrotactile feedback is capable of rendering and/or augmenting several tactile sensations (e.g., pressure, stiffness, slipperiness) and elicit multiple diverse perceptual processes pertinent to spatial, temporal, kinesthetic (e.g., directional motion), and textural (e.g., roughness) perception [24]. Electrotactile feedback directly stimulates the nerve endings of afferent nerves [13, 22]. The diverse tactile sensations are rendered by manipulating the electrical properties such as the amplitude, the frequency, and the pulse width of the electrical current [21, 24, 30].

While the studies from the relevant literature report that they have effectively rendered comparable haptic information (e.g., direction or speed), the mappings and architectures of the electrical stimulation substantially differ amongst them [24, 55]. As a result, there is a vast amount of different approaches that cannot be transferred to other applications and/or be further evaluated and compared for determining the suitability of each one. In VR, the interactions with the virtual enviroment are substantially diverse and they demand correspondingly diverse haptic requirements. Thus, the suitability of each electrotactile pattern has to be appraised in context of a certain interaction. Considering the shared electrical properties, we propose a taxonomy of the electrical stimulation mappings into larger groups (e.g., "families") that can be evaluated for specific interactions. Towards this direction, the study presented in this work examined how different electrotactile actuation parameters can be used to render different tactile sensations and how these are perceived while performing certain single bare-finger interactions in VR. Specifically, our contributions are (1) a closed loop feedback architecture to design electrotactile effects (EFX), (2) the design, evaluation, and comparison of 6 electrotactile effects for single bare finger interactions in VR and (3) evidence that EFX suitability is proportional to their congruence with the interaction being performed in VR.

2 RELATED WORK

Electrotactile feedback has been extensively used in the field of biomedical engineering (prosthesis) [24] mainly thanks to its wearability, but it has also been used, although not so extensively, in the field of teleoperation/telepresence [31, 33, 34] and VR [14, 42, 44, 51]. In this section, we briefly summarize how electrotactile feedback has been used for: (1) rendering of physical properties, (2) displaying of patterns and shapes, and (3) rendering/augmentation of objects, (for a review, see [24]).

2.1 Forces and Contact Information

In the context of the closed loop interaction control with prosthetic hands, the most common usage is the rendering of forces as pressure and sliding feedback. In this regard, the most common feedback design is the modulation of the pulse width [6, 48, 49], or amplitude [5] to convey them as an increase of the strength of the tactile sensation. Moreover, to represent the sliding velocity of the falling object, such methods also consider the change of active pads, by modulating the time interval between each pad's activation.

An alternative to this encoding is the discretization of grasping force, which is represented by using distinguishable patterns. For example, the work from [15, 41] explored the use of spatial encoding among 16 pads to represent 6 different force levels. Alternatively, Li et al. [25] explored the use of different values for amplitude, pulse width and frequency to represent 3 levels of forces for each of the 3 available pads (9 levels in total). For the latter, finding the right combination of parameters to obtain 9 differentiable levels took between 30-40 min per participant. Yet another encoding was used by Damian et al. [9], where frequency modulation was used to represent the slip speed of an object when grasped, i.e. the electrical stimulation was active when the grasping force was not enough, and off when the participant applied the right force.

Another common use of electrotactile feedback is found in teleoperation scenarios to transmit forces. For instance, the work of [54] used frequency modulation to render excessive force applied to a force sensor as a guidance mechanism. Alternatively, Ward et al. [45] used a combination of fixed frequencies and amplitudes in conjunction with pad selection in order to encode 4 levels of pressure. Forces were applied to any of the phalanxes of the 5 fingers or the palm of a robotic hand. Pad selection determined the finger/palm being stimulated, the frequency determined the phalanx, and the amplitude determined one of the 4 levels of pressure. Moreover, Sato and Tachi [35] used pad selection among 31 pads distributed in a grid along the fingertip to represent the distribution of contact forces and based on the idea of *"tactile primary colors"* [22] in conjunction with changes to the intensity and frequency. They targeted Meissner corpuscles (RA) and Merkel cells (SAI) associated to vibration and pressure respectively in order to represent the magnitude of the force. They finally encode the direction of the force by providing a stronger stimulus at the area of the finger with a higher deformation compared to the symmetric deformation produced by a perpendicular force.

Finally, in the context of VR, Hummel et al. [14] modulated the time between pulses within a pulse burst to present a 5-level pattern for rendering contact and pressure at 8 points in the distal phalanxes. This system was tested in a VR scenario where participants had to press down buttons, switch a lever and grasp a cuboid in an on-orbit servicing context. Sagardia et al. [33] use pad selection to inform contact points during a VR training for the same context of on-orbiting servicing missions. Also, Vizcay et al. [44] used frequency and pulse width modulation to render finger interpenetration into a virtual object for accurate contact. In terms of perception, Yem et al. [50] studied the effects of the amplitude and polarity of the electrical current in the perception of pressure and vibration, finding anodic stimulation is mostly described as vibration while cathodic as a combination of pressure and vibration. Choi et al. [7] tried to render pressure and tapping sensation by superpositioning two signals with different frequencies. The high frequency signal was used for pressure which in turn used pulse width modulation for controlling the strength, whereas the low frequency signal was used for the tapping sensation.

2.2 Patterns, Shapes and Guidance

In the context of prosthetic hands, Štrbac et al. [40] proposed 6 spatial patterns and 4 frequency levels using a 16 pads electrode

to encode the degrees of freedom of a prosthetic hand (hand opening/closing, wrist pronation/supination, grasping force and wrist flexion/extension). In another work, Witteveen et al. [47] used pad selection among 8 pads placed in the longitudinal direction of the forearm to indicate the discretized opening of the prosthetic hand. Moreover, as a guidance mechanism, Yoshimoto et al. [53] used pad selection and frequency modulation to correct the orientation of a blade in a carving task.

Furthermore, in the context of sensory substitution, Liu et al. [26] used pad selection among 6 pads to render braille characters to the fingertip when this is hovered over regular text using a finger cap with a camera attached to it. Regarding feedback recognition, Franceschi et al. [11] transferred mechanical stimulation applied to an electronic skin via electrotactile feedback where participants had to recognize the shape (line, square, triangle, letters), and the position and direction of the strokes. Finally, Geng and Jensen [12] investigated the ability to recognize the location and number of pulses in electrical stimulation applied to the forearm.

2.3 Material Properties

Electrotactile feedback has also been implemented for augmenting the tactile sensation proportionally to the targeted material properties. In this direction, Withana et al. [46] augmented finger exploration thanks to their thin and feel-through electrodes, which were showcased in applications where tactile properties of physical 3D objects were augmented through frequency modulation and temporal patterns were used to augment a sketched user interface. In the same study, pad selection was also used in VR for rendering contact information. Yoshimoto et al. [52] augmented material roughness in a free finger exploration via frequency modulation. Comparably, Kitamura et al. [23] used modulation of the frequency and pad switching time to explore roughness. They found that switching time is a better discriminator for roughness.

Summary: We appreciate the vast amount of mappings that have been proposed in the extensive literature. However, as reported in [24], most of the contemporary studies on electrotactile feedback pertained mainly to biomedical engineering applications, while only few works explored the potential of such feedback in VR. In the context of prostheses, electrodes are usually placed in the forearm, while the trigger of the sensation is the force applied by the fingertips. In contrast, in the case of VR, co-location of haptic feedback is crucial, since it affects the way that users interact with virtual objects [43]. Nevertheless, Kourtesis et al. [24] showed that the positive outcomes of electrotactile feedback were replicated across disciplines, and argued that several outcomes (e.g., feeling embodiment, texture, force, and speed rendering) observed in biomedical engineering would have an applicability in and impact on VR. Though, as mentioned above, solutions should proposed that are specific to VR and its requirements.

3 TACTILE FEEDBACK ARCHITECTURE

This section provides a common definition of electrotactile effects (EFXs), as modulated by the current interaction state, i.e. contact dynamics between the user's visual representation (i.e., its avatar) and virtual objects. The objectives of such architecture are expressivity and flexibility, so as to support a wide range of interactions and leverage the potential of electrotactile feedback to generate rich tactile sensations. Indeed, electrotactile feedback enables a high level of customization at different levels, from the type of electrical stimulator and control signal, to the design, number, and placement of the electrodes. At the same time, we are also interested in rendering tactile sensations for mid-air finger interactions with virtual objects, which in turn brings additional complexity to the mapping of interactions with tactile sensations.

Figure 2 presents the overview of our proposed closed loop architecture. Whenever the user touches a virtual object, the virtual contacts between the user's hand avatar and the virtual object are characterized by a set of interaction and object material properties. These properties are then mapped to a set of electrotactile feedback parameters, whose objective is to generate meaningful and coherent tactile feedback to the user.

In the following, we discuss the considered representative interactions, materials, electrotactile parameters, and authoring process, together with a description of our experimental setup and electrotactile system.

3.1 Interaction with Virtual Objects & Tactile Parameters

The interaction between the avatar and a virtual object generates a broad range of different data. We cluster this data into two categories: data pertinent to the interaction itself (*interaction data*) and data pertinent to the object being touched (*material properties*), which can be used to customize the tactile response. The position and velocity of the collision for each contact point between the user's hand and the object are examples of *interaction data*, whereas stiffness, roughness, and temperature of the object are examples of *material properties*. In an ideal pipeline, all this data would be transformed into a device-agnostic *tactile response*.

We propose a generic interface to intermediate between the data and the tactile response elicited by a haptic device. We named this interface *tactile parameters* and corresponds to the specification of the ***strength***, ***speed***, and ***direction*** of some tactile response. These parameters were chosen when we attempted to use qualifiers to describe generic tactile sensations. As an example, touching an extremely hot object would generate a strong tactile response; forcefully pushing an object would also generate a strong response; sliding the finger over a surface would generate a tactile sensation in the opposite direction to render friction; and interacting with any object that vibrates at a certain frequency/speed would generate a tactile response at an equal speed. To handle units and magnitudes in a consistent and uniform way, we treat these parameters as normalized, i.e. a strength of 1 represents the strongest sensation capable of being rendered by the haptic device, while a strength of 0 corresponds to the weakest one.

Given that the input space of data generated during an interaction is large and unknown beforehand, we delegate the mapping between the data and the tactile parameters to the interaction designer. They also need to identify which tactile parameters are going to be used to describe the targeted sensation and how they are going to leverage the available input data. As an example, imagine that we want to render the tactile sensation when the user rubs his hand along a virtual surface. In this scenario multiple interaction

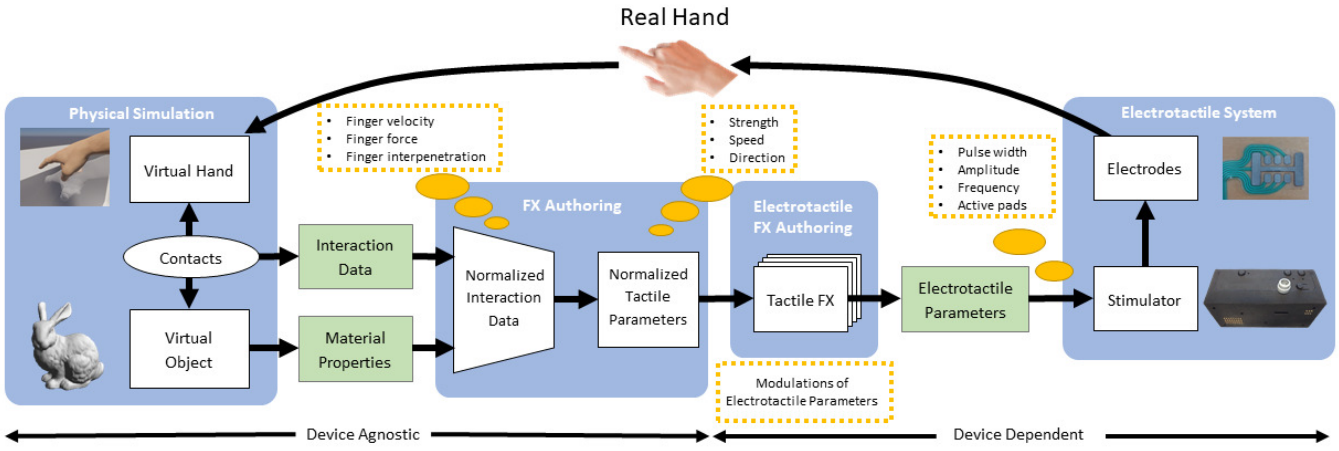

Figure 2: Architecture of the closed-loop haptic feedback. Interaction data (force, speed, etc.) is combined with the object's material properties to determine the generalized tactile parameters (strength, speed, direction), which are in turn used as input to modulate the tactile electrotactile effects (EFXs). These effects encode the actual electrical parameters that, in our case, are delivered to the user via a 2x3 electrode at the fingertip.

parameters can be considered. If we restrain ourselves to the speed of the user's motion, the speed could be mapped to the strength of the sensation. The faster the motion, the stronger the sensation. Furthermore, the material properties could also be used to enrich the tactile rendering. For example, the coupling between the speed and the roughness of the surface could be used to modulate the speed (e.g. frequency) of the sensation. The slower and the rougher the object the lower the frequency. We followed this methodology of describing the target tactile response by *strength*, *speed* and *direction* in the design of our set of electrotactile responses.

3.2 Electrotactile Stimulation Parameters

In our target scenario, the type of tactile responses we want to generate are rendered using electrical stimulation. As mentioned before, the electrical signal used for rendering our target tactile sensations can be manipulated in multiple ways.

Amplitude. It corresponds to the intensity of the electrical current and is probably the most important parameter as it is directly linked to the strength of the sensation. As each individual perceives the intensity differently at different locations, a calibration is required to accurately define the range of intensities that are perceivable while not being painful.

Polarity. Research suggests different polarity can target selectively different mechanoreceptors [22]. The perception of anodic stimulation is described as vibration whereas cathodic as vibration and pressure [50]. [19] reported that anodic stimulation is perceived as more localized and [50] reported that the strength of the sensation does not increase in the same way. Biphasic stimulation is an alternative to the monopolar one and its use has been suggested as it prevents tissue damage [3].

Waveform shape and frequency. Squared pulses are the most common signal waveform for electrotactile stimulation. The width of these pulses (pulse width, PW) is also linked to the perceived strength of the sensation, but its contribution is lower with respect to the pulse amplitude [1]. Another parameter is the frequency of the pulses which has two effects: first, it (lightly) contributes to the strength of the sensation, and, second, it drives the speed of the perceived tingles [20].

Location and number of stimulation points. This is determined by the layout of the electrode and the number of channels available in the stimulator. Multiple contact points can be stimulated independently, making possible to render rich spatio-temporal patterns.

Stimulator: We used a custom 32-channels electrical stimulator, capable of delivering squared biphasic pulses with adjustable pulse width (PW) in the range [30-500] μs, intensity, also referred as amplitude (A) between [0.1, 9] mA, and pulse frequency (f) between [1-200] Hz. The electrical stimulator delivers electrical pulses with an inter-pulse interval (IPI) of 500 μs (see Fig. 3 for a stimulation example). Pulses coming from the activation of two or more pads are delivered sequentially. However, thanks to the small IPI, those pads are perceived as stimulated at the same time in a similarly way to the time division scanning used in [35].

We used a 7-channel electrode consisting of 6 pads laid out in a 2x3 matrix used as cathodes and an anode with an H shape, as shown in the inset of Fig. 1-d.

3.3 Electrotactile Effects (EFXs)

As seen in previous work presented in Sec. 2, we observe some common strategies used for rendering rich electrotactile sensations and these include the use of pulse width, intensity or frequency modulation, spatial encoding, use of spatio-temporal patterns or modulation of hyper-parameters such as the speed at which pads are being alternated in a pattern.

Based on these common strategies, we define as *electrotactile effect* (EFX) the set of values, modulations and mappings that drives the parameters of the electrical stimulation presented in Sec. 3.2. The objective of defining EFXs is to present an abstraction layer to electrotactile stimulation, able to hide the complexity of the underlying control, focusing only on the rendered sensation and

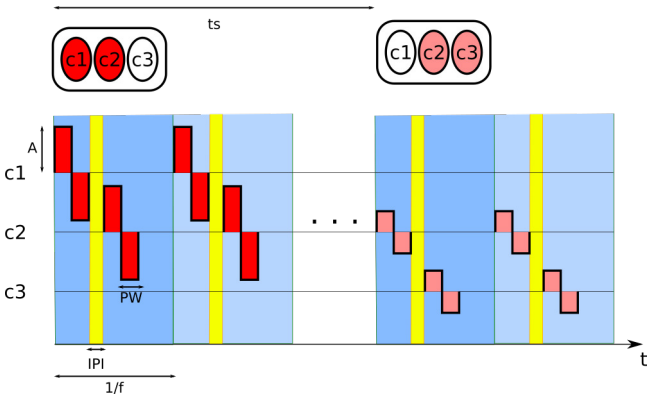

Figure 3: Example of a stimulation that uses biphasic pulses for 2 activations *ts* time apart. First activation uses *c1-c2* as active channels and the second uses *c2-c3*. Amplitude *A* of the pulses is decreased over time. Pulses separated by an inter-pulse interval (*IPI*) are perceived simultaneously. Frequency *f* of the stimulation determines the stimulation cycle where active pulses are emitted again.

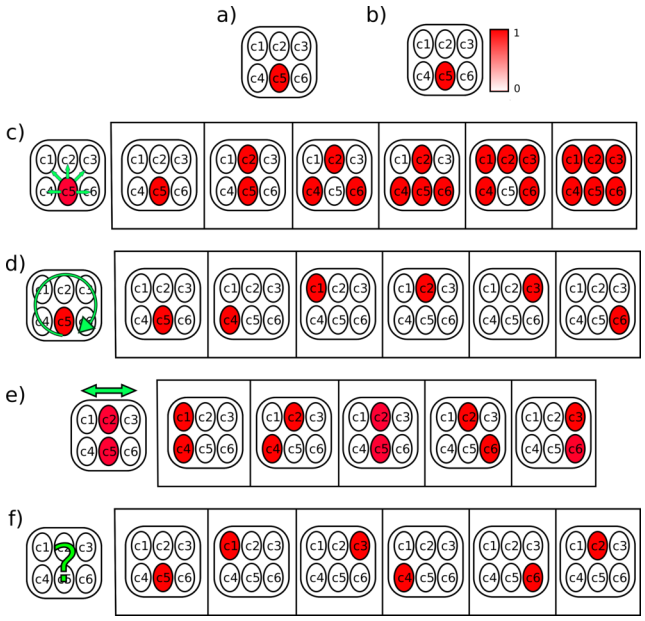

Figure 4: The six considered electrotactile effects (EFXs): a) Constant, b) Intensity Modulation, c) Spread, d) Clockwise, e) Directional, f) Random (showing a representative order).

effect with respect to the user. Inspired by the literature [24, 55], we present the implementation of six common and distinguishable effects to render interactions with virtual and remote environments. This list obtained from preliminary testing, though not exhaustive, covers a wide range of modulations and activation patterns.The implementations suggested here are examples and they are easily adapted if a different stimulator or electrode layout is used, i.e. the sensation rendered by an EFX should still be described in a similar way. EFXs are intended to be triggered once the contact between the fingertip and the virtual object is established and the stimulation should stay on until the contact breaks. We propose the following list of EFXs implemented in a 2x3 electrode (see Fig 4):

Constant *(Fig 4.a).* Its sensation is always the same regardless of user's interaction. It activates a central pad of the electrode with a fixed set of electrotactile stimulation parameters: pulse width of 150 μs, pulse frequency of 100 Hz, and amplitude set to the participant's optimal threshold for that pad (see subsubsection 4.2.2).

Intensity *(Fig 4.b).* The intensity of the sensation changes based on the user's interaction. It activates the same pad as the *constant* EFX, but the intensity of the sensation is controlled by the *strength* parameter which modulates the pulse width in a linear way between [100 - 200] μs. The pulse frequency and amplitude are the same as for *constant* EFX.

Spread *(Fig 4.c).* The number of stimulating points is controlled by the user's interaction. The number of active pads changes based on the *strength* parameter. Pads are incrementally added outwards, starting from the central bottom pad, until the 6 pads are active at the same time. To smooth the discrete increment/decrement of pads, they are added/removed by interpolating the amplitude of the stimulation between the sensation and optimal thresholds. The pulse width and frequency are the same as for *constant* EFX.

Clockwise *(Fig 4.d).* This is a spatio-temporal pattern whose speed is controlled by the user's interaction. The pads are activated following a clockwise pattern. The speed of the pattern is modulated linearly between [2-10] Hz and is determined by the *speed* parameter. The pulse width, frequency and amplitude are the same as for *constant* EFX.

Directional *(Fig 4.e).* It renders a horizontal moving sensation controlled by the user's interaction. The pads activation reacts to changes to the *direction* parameter (between -1 and 1) to switch between activations with active pads towards the left or right side of the electrode. Additionally to the change of activation, the pulse width of the active pads is also modulated between [100 - 200] μs based on the *strength* parameter.

Random *(Fig 4.f).* It renders noise by not following any activation order. It uses the same base configuration of the *clockwise* EFX but, instead of following a fixed clockwise activation order, at every pattern's cycle a random pad is selected.

3.4 Tasks & Interaction Data

Even though our architecture supports the integration of material properties into the tactile response, this study is focused on the interactions in VR. In this direction, we characterized the interactions that can be done with a single finger to test our closed loop feedback architecture, proposing the following representative tasks: **tap** the top surface of an object (see Fig. 1.a), **press down** a button (see Fig. 1.b), and **slide** horizontally across a surface (see Fig. 1.c). For all these tasks, a "physical" virtual hand (represented by the visual avatar) follows a god-object method [17] when interacting with the virtual objects, ensuring that the virtual hand do not interpenetrate virtual objects as this increases the realism of the interactions with the virtual environment.

The following *interaction data* was used to drive the *strength*, *speed*, and *direction* of the tactile response.

Interpenetration during tapping: interpenetration of the real fingertip inside the virtual object's surface representing how strongly the object has been tapped.

Compression (or force) during pressing: compression level of the button, representing how much force is being applied to it.

Velocity during sliding: fingertip velocity during the horizontal sliding action across the object's surface, representing how fast and in which direction the finger is being slid.

We mapped the finger interpenetration, the button compression level, and the sliding speed to both the *strength* and *speed* of the tactile response we wanted to elicit. For the sliding interaction, we also mapped the finger direction to the *directional* parameter of the tactile response. The details of how these values (the *interaction data*) are computed and how they are mapped to the *tactile parameters* are specified in subsubsection 4.2.1. Once these values are provided, the EFXs will produce electrotactile feedback that reacts accordingly to changes in them.

4 USER STUDY

This section describes the evaluation used to compare the coherence of the EFXs i.e. how much they match the user's expectations given the interaction being performed (tap, press, or slide). In this experiment, we are not aiming at rendering different material properties, but rather types of interactions on generic materials. In this way, participants can discern more easily between EFXs based on how they are interacting with the object and not on how the surface should be perceived. Throughout the experiment, we tried to limit any type of visual information that might hint at the material properties of the objects by using a flat gray color on them. Our objective is to analyze which EFX(s) best meets the user's expectations with respect to the considered interactions in VR.

4.1 Participants

A total of 18 participants were recruited through an in-campus advertisement, including 4 women and 14 men (age 20–35 years old), from which 15 had previous experience using haptic interfaces and 10 had already experienced electrotactile stimulation. Participants were informed of the purpose of the experiment and the general tasks they will need to perform. Following a within-subject experiment design, all participants were exposed to all six EFXs.

4.2 Apparatus

The experimental setup was composed of the electrotactile system described in Sec. 3.2 and shown in Fig. 1-d. The stimulator was attached to the forearm using an armband and the electrode was held in contact with the fingertip using Velcro, so as to ensure a stable contact throughout the experiment. We used a HTC VIVE Pro head-mounted-display and tracker to immerse the user into the virtual environment and track the position of their dominant hand. The VR application was built using the Unity3D in conjunction with the SteamVR SDK to handle the tracking and simulate the collisions. Furthermore, the bmlTux library [4] was used to define the design of the experiment (trials, repetitions, randomization). Participants interacted with the system using only their avatar's fingertip. Visual instructions were displayed in a virtual monitor in front of them. Participants were able to choose the avatar for their virtual hand based on gender and their dominant hand. We asked participants to keep the virtual hand posture during the interactions. The god-hand method was used to ensure that the virtual hand do not interpenetrate virtual objects. This was achieved by using a set of colliders that their position corresponds to the morphology of the displayed virtual hand avatar.

4.2.1 Interaction Data Processing. The **finger interpenetration**, following the god-object rendering method [17], was calculated as the offset between the visual representation of the fingertip, constrained on the surface of the object, and the true position of the fingertip obtained from the optical tracker (see offset between the solid and transparent hands in Fig. 1.a). As pilot experiments determined that users rarely experience a finger-object interpenetration larger than 5 cm, we set the range of interpenetration to [0, 5] cm, i.e., a finger interpenetration of 0 cm produces no sensation while a finger interpenetration of 5 cm (or more) during tapping produce the strongest and fastest possible tactile response.

The **compression** of the button was calculated as the offset between the current position of the button and its resting position (see offset between the solid and transparent button in Fig. 1.b). The button was designed to be compressed in the range [0, 5] cm. The button was modelled as a spring with elastic constant K=500 N/m and damping coefficient B=10 kg/s. The rigidbody to which it was attached had a mass M=50 kg. These values produced a good resistive force when pressed down using a *god-object* hand.

The finger **sliding velocity** was calculated as the velocity of the tracker projected into a vector describing the horizontal axis of the surface (see Fig. 1.c). Pilot experiments determined [0, 1.1] m/s as the common range of interest, meaning that the strongest and fastest tactile response is reached when finger's speed reaches 1.1 m/s.

4.2.2 Electrotactile Calibration. The intensity of the electrical stimulation needs to be adjusted to ensure that is well perceived but also not unpleasant. The following calibration procedure was used: for each of the six electrotactile pads on the fingertip (see Fig. 1-d), we asked users to identify their sensation threshold, i.e., the weakest perceivable stimulus, and the optimal threshold, which we defined as the maximum comfortable intensity, i.e., the strongest stimulus before it becomes uncomfortable. For safety reasons, we let the users control the delivered stimulation by dragging a slider by themselves (with no abrupt changes), so as to find these thresholds quickly without risking to deliver an uncomfortable stimulus.

As an additional confirmation step, once the two thresholds are set, we asked users to press on six virtual buttons in a VR environment. Each button activates one of the six electrode's pads, driving the delivered stimulus intensity from the lower sensation threshold (i.e., when the button is just pressed) to the optimal (maximum comfortable) threshold (i.e., when the button is fully pressed by the user). Doing so, users have the chance of testing the full range of intensity sensations they will be provided during the experiment. Users should perceive the same range of intensity sensation across the different pads, i.e., the only thing that should change when interacting with the six objects is the location of the stimulation. If this is not the case, users can re-adjust their

threshold levels, until they are satisfied and ready to proceed with the experimentation.

4.3 Experimental Tasks & Hypotheses

Participants were asked to perform the three interaction tasks, tap, press, and slide, under two evaluation modalities, **scoring** and **ranking**. In the **scoring** modality, participants performed the three tasks on an individual object in front of them and, after exposure to a certain EFX, they scored it for the given task by using a scale from 1 to 7, evaluating how coherent was the tactile sensation with respect to their actions (1: completely dissociated; 7: completely coherent). In the **ranking** modality, participants had six copies of the interactable object in front of them, each of them rendered with one of the EFXs. Participants were asked to rank the interactable objects according to how coherent was the rendered tactile sensation with respect to their actions. During both evaluations, participants could interact with the objects how many times and in which way they preferred. Inspired from previous work and our experience with electrotactile feedback, we propose the following hypotheses for each of the considered tasks:

- **[H1]** For the tapping tasks, no specific EFX will be preferred as the duration of contact is too short. Contact transient feedback will be the key in this tactile response, which is supported by all EFXs.
- **[H2]** For the pressing task, force information will be the most important. EFXs which modulate the perceived intensity (*intensity*, *spread*, and *directional* EFXs) will be preferred.
- **[H3]** For the sliding tasks, directional feedback will be most important. The *directional* EFX, which is modulated based on the finger direction and speed motion, will be preferred.

4.4 Experimental Protocol

The study followed Helsinki guidelines and it was approved by the institution's ethical committee. Upon participants' arrival, they were asked to sign a consent form explaining the experiment in detail, answered a pre-experiment questionnaire with demographics information and their familiarity with VR equipment and haptic devices. Participants were helped with putting the equipment on, which consisted of an electrode at the fingertip of the dominant hand, a tracker at the dorsal part of the same hand, an electrical stimulator at the forearm, and finally a VR head-mounted-display (see Sec. 4.2). Participants were seated in a comfortable office chair with wheels and adjustable height. Initial placement of the participant in the virtual environment was set in such a way that all interactable objects were placed at a reachable distance from the chair and at a proper height, so as to avoid any discomfort. While in VR, at the very beginning of the experience, participants calibrated the intensity of the electrical stimulation (see subsubsection 4.2.2), got familiarized with the electrotactile feedback while also confirming the right localization of the sensation, and went over a short training of the interactions with no tactile feedback to confirm they understood well the experimental tasks they need to perform.

The experiment was divided in three parts. First, participants performed the scoring task for each interaction and for each EFX. Considering that participants performed 3 repetitions for each potential combination, participants performed 54 trials within this part: 3 interactions $\times$ 6 EFXs $\times$ 3 repetitions. Trials were grouped by interaction task whose order was determined by a Latin square based on the participant's id. Within each group of trials, participants tried all six EFXs 3 times and these were presented in a random order. Before the second part of the experiment, the calibration procedure was performed again in order to make sure EFXs are rendered correctly. The second part of the experiment matched the first part. Participants scored EFXs for each task through a set of 54 trials using the same counterbalanced design. Finally, in third part of the experiment participants performed the ranking task following the same Latin-Square design.

Once participants finished the main experience, the experimenter helped them taking the equipment off and asked them to answer a post-experiment questionnaire providing additional feedback regarding the perception of the EFXs during the virtual interactions. The experiment took approximately one hour and time wise, the scoring part accounted for most of the duration of the experiment.

4.5 Results

4.5.1 Calibration Intensities. To ensure that EFXs are perceived correctly throughout the experiment, we asked participants to confirm intensities were still valid. This second calibration was done in between of the scoring trials. The intensities obtained for each calibration (first and second), for each threshold (sensation and optimal), for each pad (pad 1 to 6) are shown in Fig. 6. Differences in the *sensation threshold* were analysed using 1-way repeated measures ANOVA having the calibration part as explanatory variable. The sphericity and normality of the residuals assumptions were verified and met. All six pad presented significant differences between the two calibrations. All p-values were $< .001$ and the effect sizes ω^2 were all in the range [0.07, 0.15] 95% CI[0, 1] suggesting a medium to large effect size.

The residuals of the *optimal threshold* were not normally distributed so we performed a non-parametric paired samples Wilcoxon test between the values obtained in the first and second calibration. All pads presented significant differences with p-values $< .03$ except for pad 3 which resulted non-significant with $p = .08$.

4.5.2 Interaction EFX Coherence. We chose to run a one-way analysis for each interaction (tapping, pressing and sliding) as we are interested in evaluating the performance of EFXs per each of them. We scrutinized the data by grouping the coherence score by EFX and *experiment part* (before and after the second calibration). Even though calibration intensities were significantly different between the first and second half of the experiment, we did not find any effect between the *experiment part* and the coherence score (nor an interaction with the EFX variable). Based on this, we proceeded to analyse the score based solely on the EFX. We performed a 1-way repeated measures ANOVA on the score variable for each of the interactions having the *EFX* as explanatory variables. The normality of the residuals was examined using Shapiro-Wilk normality test and Q-Q plots. All tests suggested a normal distribution of the residuals. The sphericity assumption was tested using Mauchly Sphericity test and this was violated for all three cases. The degrees of freedom were corrected accordingly using Greenhouse-Geisser correction method. We found significant differences on the scores based on EFXs for each of the three interactions. For the tapping

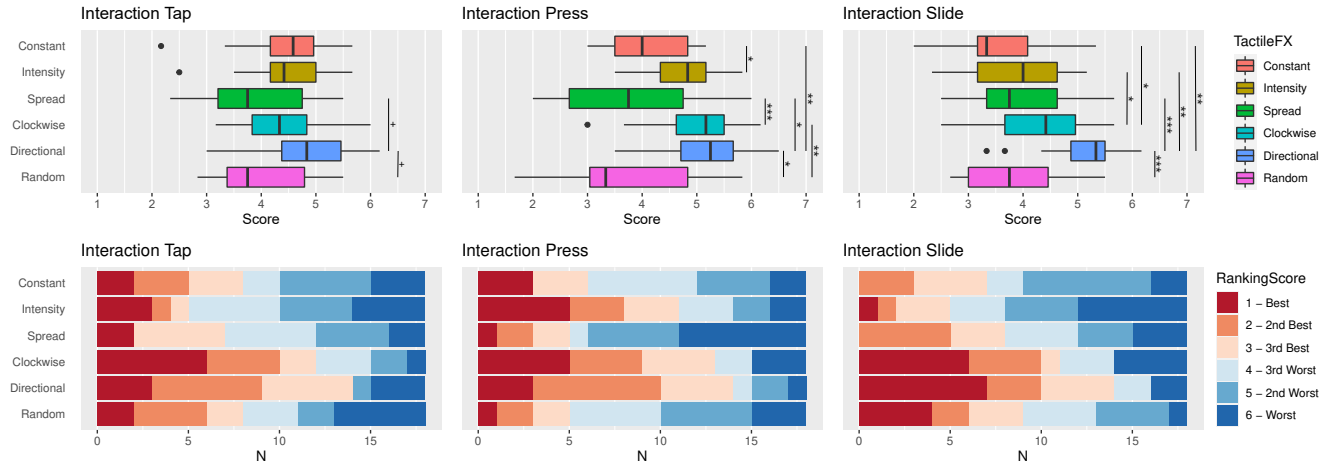

Figure 5: Distribution of scores (top) and ranking order (bottom) of the electrotactile effects (EFXs) per each interaction: tapping, pressing and sliding. Significance codes: 0 ≤ * ≤ 0.001 < ** ≤ 0.01 < * ≤ 0.05 < + ≤ 0.1.**

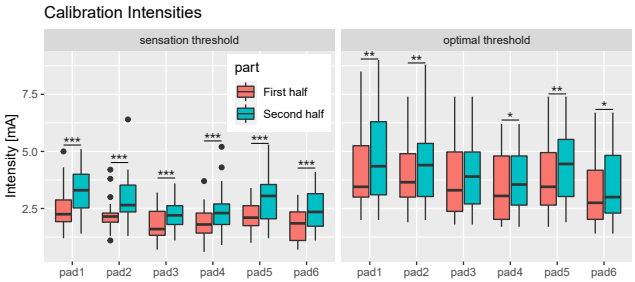

Figure 6: Intensity values for the sensation and optimal thresholds for each pads during the calibrations performed before the first and second half of the scoring trials.

interaction, ANOVA yielded (F(2.68, 45.64)=3.91, p=.017 and ω^2 = 0.09, 95% [0, 1]); for pressing (F(1.96, 33.37)=8.60, p=.001 and ω^2 = 0.22, 95% [0.07, 1]); and for sliding (F(2.43, 41.35)=10.22, p<.001 and ω^2 = 0.24, 95% [0.09, 1]). ω^2 suggests EFX has a medium to large effect size for the tapping interaction and a large effect for the pressing and sliding. We performed post-hoc pairwise comparison tests to scrutinize differences between individual EFXs. We used Bonferroni correction to amend inflated p-values due to multiple comparisons. The full list of significant differences between pair of EFXs can be seen in Fig. 5.

Tapping Task. There were no significant differences between pairs of EFXs. There were though two pair of comparisons that were close to it: the comparison between the *directional* and the *spread* EFXs ($g = 0.96, p = 0.07$) and the comparison between the *directional* and the *random* EFXs ($g = 0.91, p = 0.08$).

Pressing Task. There were multiple significant differences. We report here the most significant per EFX. the comparison between *directional* and the *constant* EFXs yielded ($g = 1.35, p = 0.007$); the *clockwise* vs *random* EFX yielded ($g = 1.02, p = 0.003$); and the *intensity* vs *constant* EFX yielded ($g = 0.96, p = 0.03$). All significance comparisons shown in Fig. 5 obtained a Hedges' g above 0.96, indicating a large effect size between EFXs.

Sliding Task. Multiple significant differences were found. We include here the most significant per EFX. The *directional* vs *random* yielded ($g = 1.23, p < .001$) and the *clockwise* vs *constant* yielded ($g = 1.07, p = .02$). Most of the differences shown in Fig. 5 obtained a Hedges' g above 1.07 except for the comparison *directional* vs *intensity* ($g = 0.51, p = .006$) and the comparison *clockwise* vs *intensity* ($g = 0.23, p = .02$).

4.5.3 EFXs Ranking. The ranking frequency can be seen in Fig. 5. Reddish stacked bars are used for the frequency of an EFX being chosen as 1st, 2nd and 3rd best EFX while bluish for 1st, 2nd and 3rd worst. We assigned $-5, -3, -1, 1, 3, 5$ points based on the ranking placement (from worst to best) and these were compared using a non-parametric Friedman test. Friedman results yielded no significant differences for tapping ($\chi^2(5) = 7.81, p = .17$); but significant for pressing ($\chi^2(5) = 14.73, p = .01$); and for sliding ($\chi^2(5) = 13.56, p = .02$). Posthoc Durbin-Conover pairwise comparisons were carried out for pressing and sliding. For pressing, comparisons between *directional*, *clockwise* and *intensity* against *spread* and *random* EFXs all obtained $p < .03$ while for sliding, comparisons between *directional* and *clockwise* against *constant*, *intensity* and *spread* EFXs obtained $p < .03$.

5 DISCUSSION

The goal of the experiment was to investigate which tactile rendering modulation/patterns are better perceived and more effective for each of the selected user-object interactions.

For the tapping task, in agreement with *[H1]*, we did not find a clear winner EFX. We only see a slight preference for the *directional* EFX when compared to the *spread* and *random* EFXs. The *directional* EFX behaves similarly to the *intensity* EFX when there is no directional data (tapping and pressing tasks) with the exception that activates two central pads rather that one (see Fig. 4-e). When there is no directional motion, the *directional* EFX only modulates

the strength of the sensation. We may theorize that participants scored the *spread* EFX badly because it elicits a strong sensation (all pads active at the same time), which might be unpleasant (especially at lateral pads where the finger seems to be more sensitive). This is supported by the verbal feedback we received from some participants, in addition to a slight score drop observed after the intensities were increased during the second calibration. Moreover, we believe that participants disliked the *random* EFX due to the noisy location offset perceived every time the object is being tapped. The ranking data is in full agreement with the score and gives a similar conclusion by also not finding any significant preference but, again, the *directional* EFX is found within the highest ranked.

For the pressing task, in line with *[H2]*, we see the *directional* and *intensity* EFXs to be within the best scored EFXs. However, in disagreement with *[H2]*, we also found the *spread* EFX to be one of the worst. We suggest the same reason described above (sensation is too strong), which is in this case even more pronounced given that the pressing interaction last longer and allows for more exploration when trying to fully compress the button. We also found the *clockwise* as one of the preferred EFXs, which was not envisaged in our hypothesis. We may theorize that participants found the modulation of the pattern's speed in conjunction with the activation sequence to be a good mechanism to inform about the state of the interaction, i.e., the compression of the button for this case. We remark that *clockwise* and *random* EFXs share the same modulation technique (changing the speed of the activation) and they only differ in how to determine the next pad to activate. The low score obtained by the *random* EFX tells us that the modulation alone was not the reason of the success of the *clockwise* EFX. As expected, the best EFXs based on the coherence score match the best EFXs based on the ranking.

For the sliding task, in accordance with *[H3]*, we see the *directional* EFX as a clear winner, with a significant higher score than all other EFXs. The only exception is with respect to the *clockwise* EFX, which still performs worse than the *directional* EFX but of a lesser extent. This is of no surprise, as the *directional* EFX is the only EFX that uses the direction data from the interaction. What is surprising, though, is the fact that the *clockwise* EFX was also scored well, even though the direction of the pattern is predefined and does not react to the changes in the sliding direction. Moreover, when taking the ranking data into account, we do not only see the *directional* and *clockwise* EFXs as suitable EFXs, but also the *random* EFX, although at a lower degree. This highlights the importance of rendering a moving sensation during sliding interactions, even when the moving direction of the sensation does not match the direction of the finger's movement. Participants verbally reported that moving EFXs were perceived coherently while sliding their finger, despite the direction mismatch, as the moving sensation was perceived as roughness.

In overall, we appreciate from all three tasks that the *directional* EFX is consistently the best and that can be used in multiple scenarios, which is expected as it is a richer EFX leveraging additional input when this is available. For cases when there is no directional information, we believe that *directional* EFX outperformed *intensity* EFX, as using two pads instead of one could have helped participants perceiving the modulation without eliciting any extra discomfort. We also believe that clear symbolic spatial information, as in the case of the *clockwise* EFX, might be easily perceived by participants and they might have relied more on it. Regarding the low score obtained by the *spread* EFX, which was attributed to the strength of the sensation being too strong when multiple pads are active, we believe adding a decreasing pulse width modulation could help compensating the added strength, making the EFX encoding solely spatial information for the area of contact.

Finally, we would like to remark the importance of assuring the consistency and quality of the feedback over time. As seen in the analysis of the calibration of the intensities, the perception of the feedback decreases over time and re-calibrations are needed along the experiment. Feedback decreases either by feedback familiarization or other factors, such as perspiration or quality of contact with the skin [24]. Calibration is an open issue and some efforts have been done in order to automatize this process [16].

6 CONCLUSION AND FUTURE WORK

This paper presented a unified architecture for rendering tactile sensations via electrotactile feedback. We reviewed the most common electrotactile modulations/patterns/effects, highlighting the lack of holistic approach when designing electrotactile effects in VR. Based on our analysis, we proposed six representative implementations leveraging electrotactile feedback in order to render tactile sensations during common finger-based interactions in VR. We conducted a user study evaluating the coherence of the proposed EFXs by means of subjective scoring and direct comparison via ranking. Our study found no preference during fast and short interactions (tapping); a preference for EFXs that render either dynamic intensities or spatio-temporal information during continuous pressing interactions (pressing) and a preference for EFXs that render moving sensations during lateral exploration (sliding). Our findings highlight the utility of the proposed rendering pipeline for designing diverse EFXs, as well as the versatility of electrotactile feedback and its efficiency in rendering tactile informations.

However, this work presents a number of limitations which would merit further research. First, the proposed architecture accounts for a wider variety of interaction parameters others than strength, speed and direction. Second, further experiments should include EFXs based on pulse frequency modulation or changes to the polarity of the signal. Although we tried to include in our comparison as many distinct and unique EFXs as we could, it was unfeasible to cover all potential modulations in a single study. Changes in polarity were not explored due to hardware limitations whereas pulse frequency modulation was intentionally left out from the experiment as we believe it is a good candidate to render material properties (e.g. roughness). Finally, we would like to study more complex multi-finger interactions which can be studied following the same approach and to what extend electrotactile sensations can replicate properties of real objects.

Despite the highlighted limitations, we believe that the proposed architecture and insights on electrotactile feedback pave the way towards an holistic tactile rendering approach to render rich tactile sensations in VR.

ACKNOWLEDGMENTS

This work was supported by the European Union's Horizon 2020 research and innovation program under grant agreement No. 856718 (TACTILITY).

REFERENCES

[1] Aiello, G. L. Multidimensional electrocutaneous stimulation. *IEEE Trans. Rehabilitation Eng. 6*, 1 (1998), 95–101.

[2] Augstein, M., and Neumayr, T. A Human-Centered Taxonomy of Interaction Modalities and Devices. *Interacting with Computers 31*, 1 (2019), 27–58.

[3] Baker, L. L., Wederich, C., McNeal, D. R., Newsam, C. J., and Waters, R. L. *Neuro muscular electrical stimulation: a practical guide.* 2000.

[4] Bebko, A. O., and Troje, N. F. bmlTUX: Design and control of experiments in virtual reality and beyond. *i-Perception 11*, 4 (2020).

[5] Chai, G., Briand, J., Su, S., Sheng, X., and Zhu, X. Electrotactile Feedback with Spatial and Mixed Coding for Object Identification and Closed-loop Control of Grasping Force in Myoelectric Prostheses. In *Proc. Annual Intl. Conf. IEEE Engineering in Medicine and Biology Society, EMBS* (2019), pp. 1805–1808.

[6] Cheng, S., Yi, A., Tan, U. X., and Zhang, D. Closed-Loop System for Myoelectric Hand Control Based on Electrotactile Stimulation. In *Proc. 3rd Intl. Conf. Advanced Robotics and Mechatronics* (2019), pp. 486–490.

[7] Choi, K., Kim, P., Kim, K. S., and Kim, S. Mixed-modality stimulation to evoke two modalities simultaneously in one channel for electrocutaneous sensory feedback. *IEEE Trans. Neural Systems and Rehab. Eng. 25*, 12 (2017), 2258–2269.

[8] Choi, S., and Kuchenbecker, K. J. Vibrotactile display: Perception, technology, and applications. *Proceedings of the IEEE 101*, 9 (2012), 2093–2104.

[9] Damian, D. D., Arita, A. H., Martinez, H., and Pfeifer, R. Slip speed feedback for grip force control. *IEEE Trans. Biomedical Engineering 59*, 8 (2012), 2200–2210.

[10] De Tinguy, X., Pacchierotti, C., Marchal, M., and Lécuyer, A. Enhancing the stiffness perception of tangible objects in mixed reality using wearable haptics. In *Proc. IEEE Conference on Virtual Reality and 3D User Interfaces (VR)* (2018), pp. 81–90.

[11] Franceschi, M., Seminara, L., Pinna, L., Valle, M., Ibrahim, A., and Dosen, S. Towards the integration of e-skin into prosthetic devices. In *12th Conference on Ph.D. Research in Microelectronics and Electronics, PRIME* (2016), pp. 1–4.

[12] Geng, B., and Jensen, W. Human ability in identification of location and pulse number for electrocutaneous stimulation applied on the forearm. *Journal of NeuroEngineering and Rehabilitation 11*, 1 (2014), 97.

[13] He, K., Yu, P., Li, M., Yang, Y., and Liu, L. The quantitative evaluation of electrotactile stimulation mode. In *Proc. IEEE Intl. Conf. Real-time Computing and Robotics (RCAR)* (2016), pp. 346–351.

[14] Hummel, J., Dodiya, J., Eckardt, L., Wolff, R., Gerndf, A., and Kuhlen, T. W. A lightweight electrotactile feedback device for grasp improvement in immersive virtual environments. In *Proc. IEEE Virtual Reality* (2016), pp. 39–48.

[15] Isaković, M., Belić, M., Štrbac, M., Popović, I., Došen, S., Farina, D., and Keller, T. Electrotactile feedback improves performance and facilitates learning in the routine grasping task. *European Journal of Translational Myology 26*, 3 (2016), 197–202.

[16] Isaković, M., Malešević, J., Keller, T., Kostić, M., and Štrbac, M. Optimization of semiautomated calibration algorithm of multichannel electrotactile feedback for myoelectric hand prosthesis. *Applied bionics and biomechanics* (2019).

[17] Jacobs, J., Stengel, M., and Froehlich, B. A generalized god-object method for plausible finger-based interactions in virtual environments. In *Proc. IEEE Symposium on 3D User Interfaces (3DUI)* (2012), pp. 43–51.

[18] Jeunet, C., Albert, L., Argelaguet, F., and Lécuyer, A. "Do you feel in control?": towards novel approaches to characterise, manipulate and measure the sense of agency in virtual environments. *IEEE Trans. Vis. Comp. Graphics 24*, 4 (2018), 1486–1495.

[19] Kaczmarek, K. A., Tyler, M. E., and Bach-y Rita, P. Electrotactile haptic display on the fingertips: Preliminary results. In *Proc. Intl. Conf. IEEE Engineering in Medicine and Biology Society* (1994), vol. 2, pp. 940–941.

[20] Kaczmarek, K. A., Tyler, M. E., Okpara, U. O., and Haase, S. J. Interaction of Perceived Frequency and Intensity in Fingertip Electrotactile Stimulation: Dissimilarity Ratings and Multidimensional Scaling. *IEEE Trans. Neural Systems and Rehabilitation Eng. 25*, 11 (2017), 2067–2074.

[21] Kajimoto, H. *Electro-tactile Display: Principle and Hardware.* 2016, pp. 79–96.

[22] Kajimoto, H., Kawakami, N., Maeda, T., and Tachi, S. Electro-tactile display with tactile primary color approach. *Graduate School of Information and Technology, The University of Tokyo* (2004).

[23] Kitamura, N., and Miki, N. Micro-needle-based electro tactile display to present various tactile sensation. In *Proc. IEEE Intl. Conf. Micro Electro Mechanical Systems (MEMS)* (2015), vol. 2015, pp. 649–650.

[24] Kourtesis, P., Argelaguet, F., Vizcay, S., Marchal, M., and Pacchierotti, C. Electrotactile feedback applications for hand and arm interactions: A systematic review, meta-analysis, and future directions. *IEEE Trans. Haptics* (2022), 1–18.

[25] Li, K., Boyd, P., Zhou, Y., Ju, Z., and Liu, H. Electrotactile Feedback in a Virtual Hand Rehabilitation Platform: Evaluation and Implementation, 2018.

[26] Liu, Z., Luo, Y., Cordero, J., Zhao, N., and Shen, Y. Finger-eye: A wearable text reading assistive system for the blind and visually impaired. In *Proc. IEEE Intl. Conf. Real-Time Computing and Robotics, RCAR* (2016), pp. 123–128.

[27] Maisto, M., Pacchierotti, C., Chinello, F., Salvietti, G., De Luca, A., and Prattichizzo, D. Evaluation of wearable haptic systems for the fingers in augmented reality applications. *IEEE Trans. Haptics 10*, 4 (2017), 511–522.

[28] Meli, L., Pacchierotti, C., Salvietti, G., Chinello, F., Maisto, M., De Luca, A., and Prattichizzo, D. Combining wearable finger haptics and augmented reality: User evaluation using an external camera and the microsoft hololens. *IEEE Robotics and Automation Letters 3*, 4 (2018), 4297–4304.

[29] Pacchierotti, C., Sinclair, S., Solazzi, M., Frisoli, A., Hayward, V., and Prattichizzo, D. Wearable haptic systems for the fingertip and the hand: Taxonomy, review, and perspectives. *IEEE Trans. Haptics 10*, 4 (2017), 580–600.

[30] Pamungkas, D. S., and Caesarendra, W. Overview electrotactile feedback for enhancing human computer interface. *Journal of Physics: Conference Series 1007* (2018), 012001.

[31] Pamungkas, D. S., and Ward, K. Tele-operation of a robot arm with electro tactile feedback. In *Proc. IEEE/ASME Intl. Conf. Advanced Intelligent Mechatronics: Mechatronics for Human Wellbeing, AIM 2013* (2013), pp. 704–709.

[32] Rakkolainen, I., Farooq, A., Kangas, J., Hakulinen, J., Rantala, J., Turunen, M., and Raisamo, R. Technologies for multimodal interaction in extended reality: A scoping review. *Multimodal Technologies and Interaction 5*, 12 (2021).

[33] Sagardia, M., Hertkorn, K., Hulin, T., Schätzle, S., Wolff, R., Hummel, J., Dodiya, J., and Gerndt, A. VR-OOS: The DLR's virtual reality simulator for telerobotic on-orbit servicing with haptic feedback. In *Proc. IEEE Aerospace Conference* (2015), pp. 1–17.

[34] Sato, K., Shinoda, H., and Tachi, S. Design and implementation of transmission system of initial haptic impression. In *Proc. SICE Annual Conference* (2011), pp. 616–621.

[35] Sato, K., and Tachi, S. Design of electrotactile stimulation to represent distribution of force vectors. In *Proc. IEEE Haptics Symposium* (2010), pp. 121–128.

[36] Scheggi, S., Meli, L., Pacchierotti, C., and Prattichizzo, D. Touch the virtual reality: using the leap motion controller for hand tracking and wearable tactile devices for immersive haptic rendering. In *Proc. ACM SIGGRAPH Posters.* 2015.

[37] Skarbez, R., Brooks, Jr, F. P., and Whitton, M. C. A survey of presence and related concepts. *ACM Computing Surveys (CSUR) 50*, 6 (2017), 1–39.

[38] Slater, M. Place illusion and plausibility can lead to realistic behaviour in immersive virtual environments. *Philosophical Transactions of the Royal Society B: Biological Sciences 364*, 1535 (2009), 3549–3557.

[39] Spagnoletti, G., Meli, L., Baldi, T. L., Gioioso, G., Pacchierotti, C., and Prattichizzo, D. Rendering of pressure and textures using wearable haptics in immersive VR environments. In *Proc. IEEE Conference on Virtual Reality and 3D User Interfaces (VR)* (2018), pp. 691–692.

[40] Štrbac, M., Belić, M., Isaković, M., Kojić, V., Bijelić, G., Popović, I., Radotić, M., Došen, S., Marković, M., Farina, D., and Keller, T. Integrated and flexible multichannel interface for electrotactile stimulation. *Journal of Neural Engineering 13*, 4 (2016), 046014.

[41] Štrbac, M., Isaković, M., Belić, M., Popović, I., Simanić, I., Farina, D., Keller, T., and Došen, S. Short-and long-term learning of feedforward control of a myoelectric prosthesis with sensory feedback by amputees. *IEEE Trans. Neural Systems and Rehabilitation Eng. 25*, 11 (2017), 2133–2145.

[42] Sutopo Pamungkas, D. Enhancing human computer interaction with electrotactile feedback. In *University of Wollongong Thesis* (2016).

[43] Swapp, D., Pawar, V., and Loscos, C. Interaction with co-located haptic feedback in virtual reality. *Virtual Reality 10*, 1 (2006), 24–30.

[44] Vizcay, S., Kourtesis, P., Argelaguet, F., Pacchierotti, C., and Marchal, M. Electrotactile Feedback For Enhancing Contact Information in Virtual Reality. In *Proc. Intl. Conf. Artificial Reality and Telexistence and Eurographics Symposium on Virtual Environments (ICAT-EGVE)* (2021), p. 10.

[45] Ward, K., and Pamungkas, D. Multi-channel electro-tactile feedback system for a prosthetic hand. *Mechatronics and Machine Vision in Practice 3* (2018), 181–193.

[46] Withana, A., Groeger, D., and Steimle, J. Tacttoo: A thin and feel-through tattoo for on-skin tactile output. In *UIST - Proc. 31st Annual ACM Symposium on User Interface Software and Technology* (2018), pp. 365–378.

[47] Witteveen, H. J. B., Droog, E. A., Rietman, J. S., and Veltink, P. H. Vibro- and electrotactile user feedback on hand opening for myoelectric forearm prostheses. *IEEE Trans. Biomedical Engineering 59*, 8 (2012), 2219–2226.

[48] Xu, H., Bao, L., Zhang, D., and Zhu, X. Identify key grasping-related properties based on cutaneous electrotactile stimulation. In *Proc. IEEE 19th International Functional Electrical Stimulation Society Annual Conference* (2014).

[49] Xu, H., Zhang, D., Huegel, J. C., Xu, W., and Zhu, X. Effects of Different Tactile Feedback on Myoelectric Closed-Loop Control for Grasping Based on Electrotactile Stimulation. *IEEE Trans. Neural Systems and Rehabilitation Eng. 24*, 8 (2016), 827–836.

[50] Yem, V., and Kajimoto, H. Comparative Evaluation of Tactile Sensation by

Electrical and Mechanical Stimulation. *IEEE Trans. Haptics 10*, 1 (2017), 130–134.

[51] Yem, V., Vu, K., Kon, Y., and Kajimoto, H. Effect of Electrical Stimulation Haptic Feedback on Perceptions of Softness-Hardness and Stickiness while Touching a Virtual Object. In *Proc. IEEE Conference on Virtual Reality and 3D User Interfaces* (2018), pp. 89–96.

[52] Yoshimoto, S., Kuroda, Y., Imura, M., and Oshiro, O. Material roughness modulation via electrotactile augmentation. *IEEE Trans. Haptics 8*, 2 (2015), 199–208.

[53] Yoshimoto, S., Kuroda, Y., Imura, M., Oshiro, O., Nozaki, K., Taga, Y., Machi, H., and Tamagawa, H. Electrotactile Augmentation for Carving Guidance. *IEEE Trans. Haptics 9*, 1 (2016), 43–53.

[54] Yoshimoto, S., Kuroda, Y., Imura, M., Oshiro, O., and Sato, K. Electrically multiplexed tactile interface: Fusion of smart tactile sensor and display. In *Proc. World Haptics Conference* (2013), pp. 151–156.

[55] Zhou, Z., Yang, Y., Liu, J., Zeng, J., Wang, X., and Liu, H. Electrotactile perception properties and its applications: A review. *IEEE Trans. Haptics* (2022).